JACC: CARDIOVASCULAR IMAGING VOL. 12, NO. 3, 2019

PUBLISHED BY ELSEVIER

iREVIEW

STATE-OF-THE-ART PAPER

Anatomy and Physiology of the Tricuspid Valve

Abdellaziz Dahou, MD, PhD,[a,b] Dmitry Levin, BA,[c] Mark Reisman, MD,[c] Rebecca T. Hahn, MD[a,b]

SUMMARY

An appreciation of the complex and variable anatomy of the tricuspid valve is essential to unraveling the pathophysiology of tricuspid regurgitation. A greater appreciation of normal and abnormal anatomy is important as new methods of treating the tricuspid regurgitation are developed. This review of tricuspid valve and right heart anatomy is followed by a discussion of the possible pathophysiology of secondary (functional) tricuspid regurgitation. (J Am Coll Cardiol Img 2019;12:458-68) © 2019 by the American College of Cardiology Foundation.

With the recognition of the impact of tricuspid regurgitation (TR) on outcomes in a number of disease states (1-5), interest in understanding this disease process has grown. To help understand the pathophysiology of TR and the role of interventions in treatment of the disease, an appreciation of the complex and variable anatomy of the tricuspid valve (TV) is essential (6-12). This paper reviews tricuspid and right heart anatomy, discusses the pathophysiology of secondary TR, summarizes the anatomic structures relevant to interventional procedures.

ANATOMY AND FUNCTION OF THE TRICUSPID VALVE

The TV is the largest and most apically positioned of the 4 cardiac valves (**Figure 1**) with a normal orifice area between 7 and 9 cm^2 (9). Because of its large size and the low pressure differences between the right atrium (RA) and right ventricle (RV), peak transtricuspid diastolic velocities are typically lower than 1 m/s with mean gradients of <2 mm Hg (9). Similar to the mitral valve, the TV can be divided into 4 components: the leaflets, the papillary muscles, the chordal attachments, and the annulus (with attached atrium and ventricle) (7,12-16). The leaflets and their relationship to the chordae and papillary muscle play an important role in TV closure during systole but also may be integrally related to RV size and function.

TRICUSPID VALVE LEAFLETS. Although the TV is typically composed of 3 leaflets of unequal size, in many cases, 2 (bicuspid) or more than 3 leaflets may be present as anatomic variants in healthy subjects (6,9) (**Figure 2**). When described relative to their anatomic position in the body (attitudinally appropriate nomenclature), the 3 leaflets would be the septal, anterior-superior, and inferior leaflets (7). Typically, however, these leaflets are referred to as the septal, anterior, and posterior leaflets, respectively. The anterior leaflet (**Figure 3A**) is generally the largest and the longest in the radial direction, with the larger area and the greatest motion. The posterior leaflet may have multiple scallops and is the shortest circumferentially. It may not be clearly separated from the anterior leaflet in approximately 10% of patients. The septal leaflet (**Figure 3B**) is the shortest

From the [a]NewYork-Presbyterian/Columbia University Irving Medical Center, New York, New York; [b]Cardiovascular Research Foundation, New York, New York; and the [c]University of Washington Medical Center, Seattle, Washington. This research was not supported by public, commercial, or not-for-profit sectors. Dr. Hahn is the Chief Scientific Officer for the Echocardiography Core Laboratory at the Cardiovascular Research Foundation for which she receives no direct industry compensation; and has received personal fees from Abbott Vascular, Boston Scientific, Bayliss, Navigate, Philips Healthcare, and Siemens Healthineers. All other authors have reported that they have no relationships relevant to the contents of this paper to disclose.

Manuscript received May 25, 2018; revised manuscript received July 11, 2018, accepted July 12, 2018.

ISSN 1936-878X/$36.00 https://doi.org/10.1016/j.jcmg.2018.07.032

in the radial direction and the least mobile. It is attached to the tricuspid annulus directly above the interventricular septum (17), with many third-order chordae that may be attached directly to the septum (6,7,9); it is inserted into the septum ≤10 mm apically to the septal insertion of the anterior mitral leaflet (i.e., apically displaced) (9). Anatomic landmarks for each leaflet vary significantly depending on the size and shape of the annulus; however, the commissure between the septal and posterior leaflets (which are always clearly separated) is usually located near the entrance of the coronary sinus to the right atrium (**Figure 4**). The noncoronary sinus of Valsalva of the aortic root will typically be adjacent to the commissure between the septal and anterior leaflets. Because the anterior and septal leaflets are usually the largest circumferentially, the anteroseptal commissure is the longest. Coaptation of the TV normally is located at the level of the annulus or just below it, with a coaptation length of 5 to 10 mm (18). This excess coaptation length functions as the coaptation reserve, allowing some dilation of the annulus before malcoaptation occurs.

TRICUSPID VALVE TENSOR APPARATUS. The papillary muscles and chordae form the "tensor apparatus" of the tricuspid valve (19). There are 2 distinct papillary muscles (anterior and posterior) and a third variable papillary muscle. The largest muscle is typically the anterior papillary muscle with chordae supporting the anterior and posterior leaflets (**Figure 3A**). The moderator band may join this papillary muscle. The posterior papillary muscle, which is often bifid or trifid, lends chordal support to the posterior and septal leaflets. The septal papillary muscle is variable: it may be small or multiple or even absent in up to 20% of normal patients. Chordae may arise directly from the septum to the anterior and septal leaflets (**Figure 3B**). Accessory chordae may attach to the right ventricular free wall as well as to the moderator band. Thus 2 leaflets of the TV (septal and anterior) are connected to the interventricular septum, and 2 leaflets (anterior and posterior) are dependent upon a large anterior papillary muscle along the anterolateral RV wall. Because of the fixed length of the chordae, displacement of either the RV septal or lateral wall positions will affect tricuspid leaflet coaptation.

Chordae of the TV are fibrous cords of various lengths that connect the papillary muscles to the tricuspid valve leaflets. Chordae tendineae are approximately 80% collagen, whereas the remaining 20% is made of elastin and endothelial cells. In a study including 50 normal tricuspid valves (18), 5 types of chordae were distinguished by their morphology and mode of insertion: fan-shaped, rough zone, basal, free edge, and deep chordae. The last 2 types are unique to the tricuspid valve. The number of chordae varied from 17 to 36 with an average of 25 chordae.

In addition to the true chordae described above that insert into the leaflet tissue, false chordae inset elsewhere and can connect 2 papillary muscles or a papillary muscle to the ventricular wall, or they may connect points on the ventricular walls. True chordae typically originate from the apical third of the papillary muscle but can originate from the ventricular walls, as is the case for the septal leaflet (18,20). From an interventional perspective, the chordae may interact with catheters and devices, causing additional difficulties and challenges during transcatheter approaches for the TV. In addition, the mechanical properties and ultrastructure of normal human tricuspid valve chordae tendineae consist of fairly straight collagen bundles that are made of networks of collagen fibrils and thus exhibit less extensibility than normal mitral valve chordae of comparable size (21). This may help explain the marked tethering that occurs with dilation of the RV or displacement of the papillary muscles.

TRICUSPID VALVE ANNULUS. Although the term annulus implies a distinct, fibrous structure, the pathology study of 12 cadaveric normal right hearts by Messer et al. (22) suggested this is a misnomer. The normal tricuspid annulus is D-shaped (**Figure 4A**) and nonplanar with 2 distinct segments: a larger C-shaped segment that corresponds to the free wall of the RA and the RV; and a shorter, relatively straight segment that corresponds to the septal leaflet and the ventricular septum. On gross examination, there are multiple muscular bars measuring approximately 2 to 4 mm in diameter in the annulus itself, from the free wall of the RV and the septal wall, frequently in a crisscross pattern (**Figure 4B**). These muscle bands may offer support to the nonfibrous RA-RV junction. However, their roles in dilation of the annulus with RV dilation are unknown. On histologic examination, there appears to be very little fibrous tissue or collagen along the RV free wall segment; rather, the annulus is composed of epicardium and endocardium on either side (**Figure 4C**), with the coronary artery and veins with surrounding adipocytes in the atrioventricular groove. In 6 of the 12 hearts there was an insignificant amount of fibrous tissue in the septal segment annulus (22). In some hearts, the base of the tricuspid valve was seen to be entirely an atrial structure (22).

ABBREVIATIONS AND ACRONYMS

RA = right atrium

RV = right ventricle

STR = secondary tricuspid regurgitation

SVC = superior vena cava

TR = tricuspid regurgitation

TV = tricuspid valve

JACC: CARDIOVASCULAR IMAGING, VOL. 12, NO. 3, 2019
MARCH 2019:458–68

FIGURE 1 Gross Anatomy of the TV

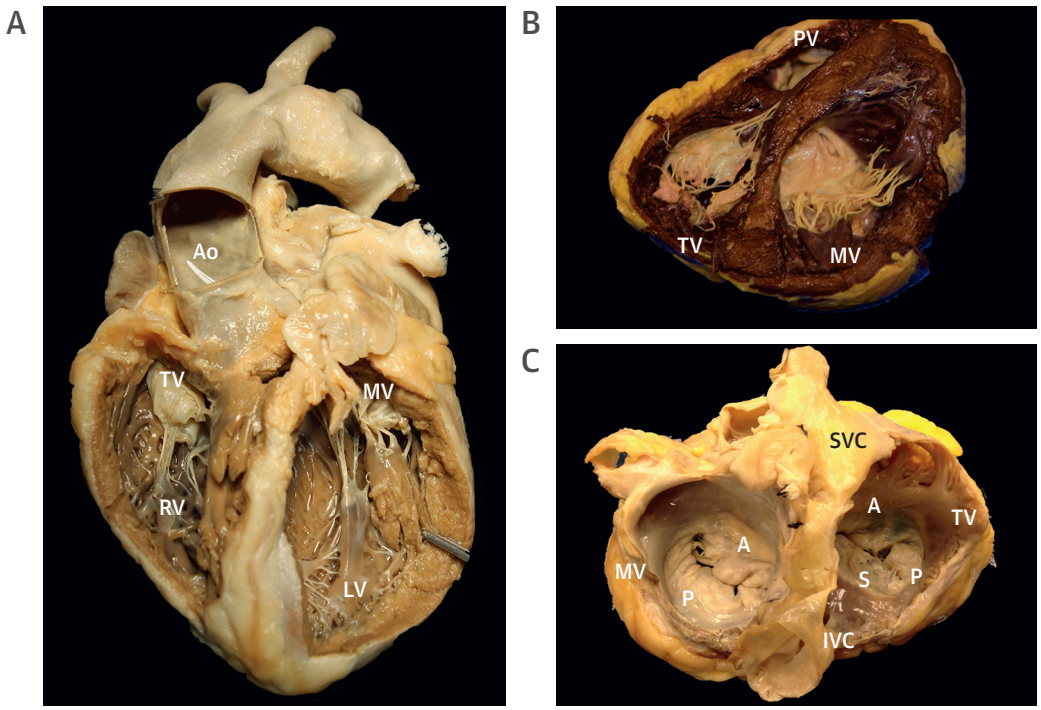

(A) Relationship of the TV to the left heart structures. Although typically shown in this orientation, the TV actually is the most anterior and apical of the 4 cardiac valves. **(B)** Relationship of the TV to the right ventricular outflow tract and the PV. Of note, there is no fibrous continuity between these 2 valves. **(C)** Relative position of the TV from the atrial aspect. A = anterior leaflet; Ao = aorta; IVC = inferior vena cava; LV = left ventricle; MV = mitral valve; P = posterior leaflet; PV = pulmonic valve; S = septal leaflet; SVC = superior vena cava; TV = tricuspid valve.

The tricuspid annulus is a dynamic structure with significant changes in its area (up to ~30%) during the cardiac cycle and is larger at end systole/early diastole and during atrial systole (9) and also under loading conditions. Normal tricuspid annular circumferences and areas in healthy subjects are 12 ± 1 cm and 11 ± 2 cm^2, respectively, as measured by 3D echocardiography (9,12,23). Unlike the mitral valve annulus, the tricuspid valve annulus may be difficult to define on surgical or anatomic inspection; the anterior annulus is less well defined than the posterior annulus. The posteroseptal tricuspid annulus is more ventricular, and the anteroseptal portion is more atrial (8,24). With secondary TR, the tricuspid annulus dilates toward the lateral and posterior free wall and becomes more spherical and planar (25). Dilation of the septal segment is limited because of its anatomic relation with the fibrous skeleton of the heart (10).

ADJACENT ANATOMY. Finally, 3 important structures lie in close proximity to the tricuspid valve (**Central Illustration**). The noncoronary sinus of Valsalva is adjacent to the commissure between the anterior and septal leaflets. Transcatheter devices that require anchoring in this region pose the risk of aortic perforation. The atrioventricular (AV) node and the bundle of His cross the septal leaflet attachment 3 to 5 mm posterior to the anteroseptal commissure (**Figure 5**). Pressure on or perforation of the node may result in heart blockage. The right coronary artery exits the right coronary sinus of Valsalva and courses in the right AV groove posteriorly to the crux of the heart, where it takes an acute bend and continues downward in the posterior interventricular sulcus (**Figure 6**). Because a long segment of the artery resides in the AV groove, the right coronary artery can be used to indicate the approximate location of the annulus. Although the proximal portion of the right coronary artery is relatively distant from the annulus, there is a gradual shortening of the distance to the endocardial surface toward the inferior segment of the annulus to <3 mm (26), an important consideration for annulus-anchoring devices (27,28).

FIGURE 2 Variable Tricuspid Leaflets

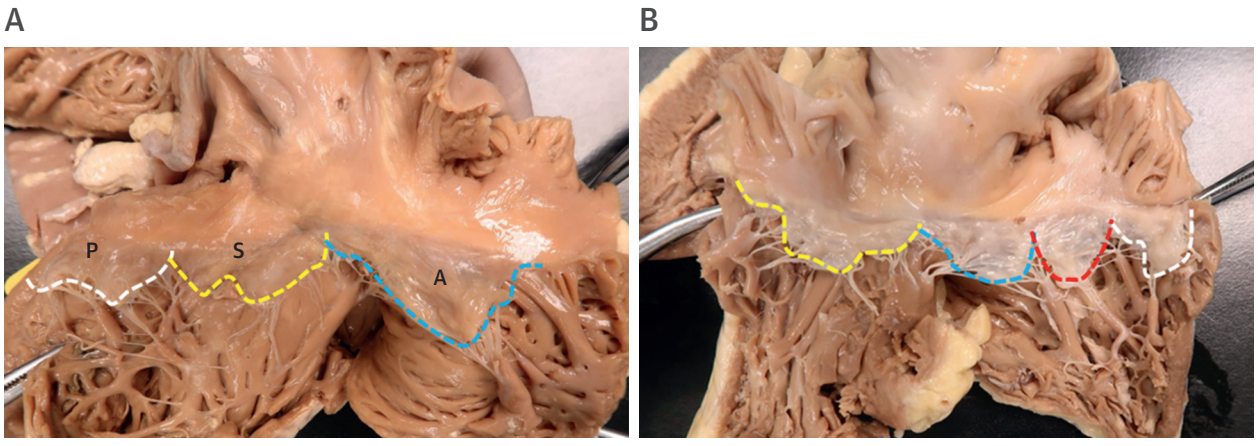

The number of tricuspid leaflets is highly variable. The most common configuration is a 3- leaflet valve **(A)**. In this figure, the **white line** indicating the P leaflet, the **yellow line** indicates the S leaflet, and the **blue line** indicates the A leaflet. Frequently, more than 3 leaflets are seen **(B)**. The **orange line (B)** represents the fourth leaflet in this quadricuspid valve. A = anterior leaflet; P = posterior leaflet; S = septal leaflet.

The superior and inferior vena cavae are other important structures related to the TV anatomy when considering transcatheter intervention for TV. They represent the ultimate access for the transcatheter approaches to the TV and may represent, in some cases, a landing zone or the site of the implanted device. The inferior vena cava is the largest vein in the human body, with a normal

FIGURE 3 Papillary Muscles

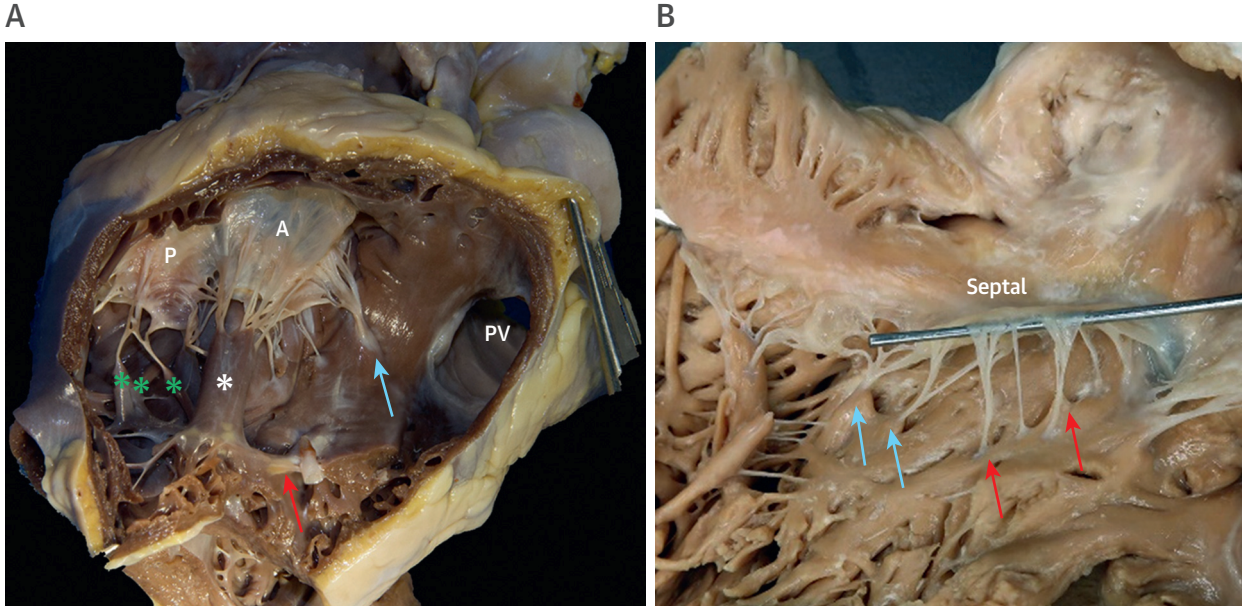

(A) Typical papillary muscle distribution for the tricuspid valve. The anterior papillary muscle is typically the largest **(white asterisk)**, which provides chordal support for the A and P leaflets. The moderator band **(orange arrows)** may join this papillary muscle. The posterior papillary muscle is often bifid or trifid **(green asterisks)** and lends chordal support to the posterior and septal leaflets. The septal papillary muscle is variable **(blue arrow)**. **(B)** Septal leaflet chordal attachments to the septal papillary muscle are shown **(blue arrows)** and directly from the septal myocardium **(orange arrows)**. Abbreviations as in Figures 1 and 2.

FIGURE 4 Tricuspid Valve Annulus

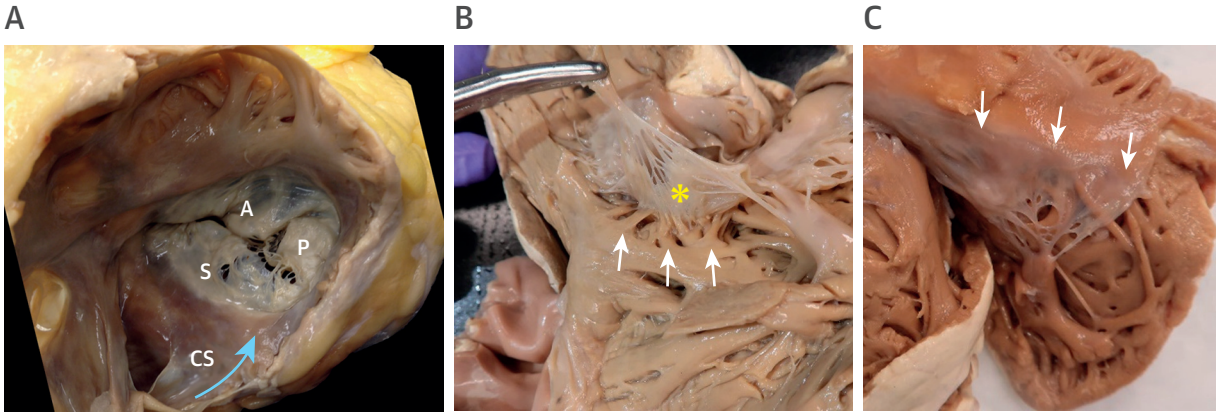

(A) The tricuspid valve is seen from the atrial side with the typically D-shaped annulus composed of a flat septal region and curved anterior and posterior regions. **(B)** The ventricular surface of the anterior leaflet **(asterisk)** with multiple "crisscrossing" muscle attachments **(arrows)** directly to the base of the leaflet. **(C)** The atrial surface of the anterior leaflet annulus **(white arrows)**, which is not fibrous and has a smooth transition from atrium to ventricle. CS = coronary sinus **(curved blue arrow)**; other abbreviations as in Figure 1.

size of usually <21 mm (29). It is formed by the joining of the left and right common iliac veins, and it is localized in the retroperitoneal cavity. It runs along the right side of the vertebral column and enters the RA at the lower right, posterior side of the heart. The superior vena cava (SVC) is formed by the confluence of the right and left brachiocephalic veins. It courses along the right middle mediastinum, with the trachea and ascending aorta on its left, and drains into the superior wall of the RA. The mean length of the SVC is 7.1 ± 1.4 cm, and its maximum diameter in adults as measured by CT angiography is 2.1 ± 0.7 cm (30,31). The SVC is often irregular in shape on

CENTRAL ILLUSTRATION Appreciating the Complex Anatomy of the TV Anatomy Is Essential to Understand the Pathophysiology of Tricuspid Regurgitation

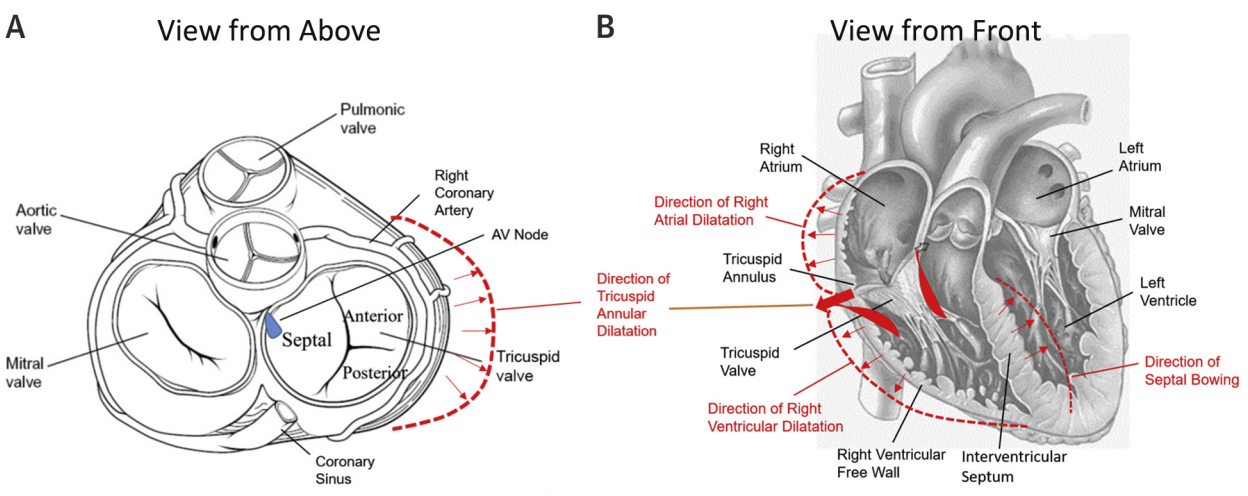

Dahou, A. et al. J Am Coll Cardiol Img. 2019;12(3):458-68.

(A) The anatomy of the tricuspid valve and adjacent structures from a surgical view. **(B)** The relevant anatomy shown from the front view. The **red dotted lines** show the direction of dilation of various structures in the setting of secondary tricuspid regurgitation.

FIGURE 5 Triangle of Koch and Membranous Septum

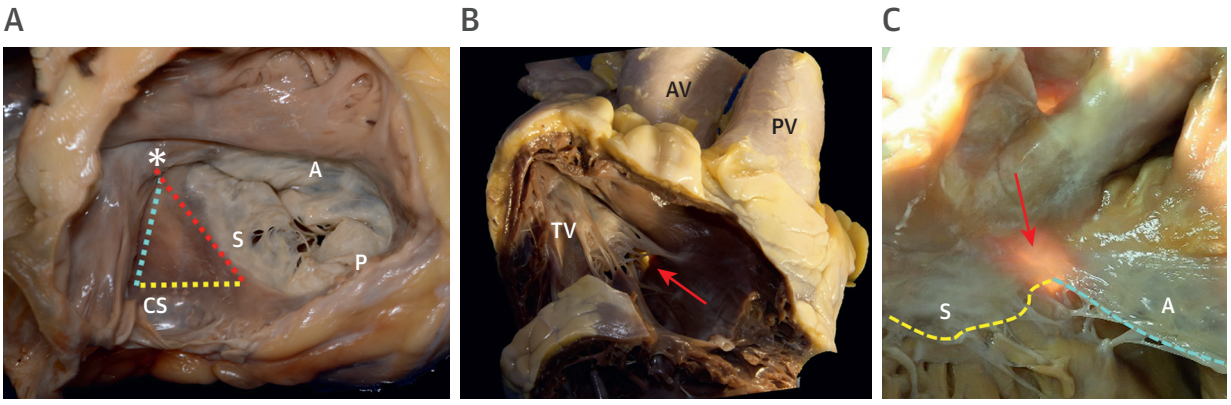

(A) The anatomic landmarks of the triangle of Koch. The tendon of Todaro **(blue line)** lies above the eustachian valve forming one side of the triangle. The hinge point of the septal leaflet **(orange line)** forms a second side, and the CS forms the base of the triangle **(yellow line)** with the apex of the triangle **(asterisk)**, marking the location of the atrioventricular conduction axis near the membranous septum. **(B)** The ventricular view and **(C)** the atrial view of the membranous septum **(orange arrow = backlit)** at the commissure between the S and and A leaflets of the tricuspid valve. AV = atrioventricular node; other abbreviations as in Figures 1 and 4.

cross-sectional images, with a normal range for the major axis of 1.5 to 2.8 cm and minor axis of 1 to 2.4 cm. An SVC area of <1.07 cm^2 is consistent with obstruction or compression (32).

ANATOMY AND FUNCTION OF THE RIGHT VENTRICLE

A number of unique features of the right ventriculoatrial anatomy help to drive flow across the TV annulus. A rotational or helical flow within the RA contributes to flow into the RV and results in conservation of atrial blood flow kinetic energy (33,34). Because of the higher surface-to-volume ratio of the RV, a smaller inward motion is required to eject the same SV as the LV. The outflow tract of the RV is anatomically distinct from the body of the RV. Thus, unlike the LV, which must use longitudinal and rotational blood flow motion to change the direction of blood flow from ventricular inflow to outflow, blood flow in the RV moves in a physiologically appropriate direction immediately on crossing the TV. Balanced longitudinal and transversal forces result in the creation of centripetal force on RV blood flow, which is aimed in early systole toward the interventricular septum and then rerouted using the main transversal axis of the RV (from diaphragm to RV outflow tract) to drive the blood toward the pulmonary valve (35).

Ventricular interdependence, along with contractility, afterload, and preload, determine RV systolic function (36,37). The RV has long been believed to be more sensitive than the LV to acute increases in afterload (38), with experimental models showing that a pressure load on the RV is less well tolerated than a volume load (39). Flow out of the RV outflow tract depends on a low-impedance, highly distensible pulmonary vascular system in order to pump the same SV as the left ventricle, although using only ~20% of LV stroke work in the resting condition. With increasing pulmonary artery pressure (PAP), there were sequential morphologic changes seen with tricuspid annular RA dilation early (i.e., in the setting

FIGURE 6 Right Coronary Artery

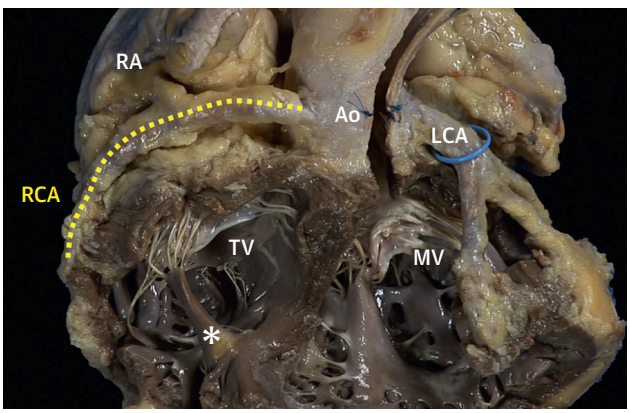

The proximal RCA exits the right coronary sinus of Valsalva of the Ao and courses in the atrioventricular groove within adipose tissue **(yellow dashed line)**. The anterior papillary muscle is marked by an **asterisk**. LCA = left coronary artery; MV = mitral valve; RA = right atrium; RCA = right coronary artery; other abbreviations as in Figure 1.

TABLE 1 Causes of Tricuspid Regurgitation

Primary TR
Congenital
Ebstein's anomaly
Tricuspid valve tethering associated with perimembranous ventricular septal aneurysm or defect
Tricuspid valve dysplasia, hypoplasia, or cleft
Double orifice tricuspid valve
Other (giant RA)
Acquired
Myxomatous degeneration (Barlow's disease): TV prolapse, flail
Endocarditis
Carcinoid syndrome
Rheumatic disease
Trauma (chest wall trauma or TV trauma following intracardiac procedures: RV intramyocardial biopsy, and so on)
Pacemaker/device-related
Secondary TR
According to the underlying disease:
Left-sided heart disease (valve disease and/or left ventricular dysfunction)
Pulmonary arterial hypertension from any cause
RV dysfunction from any cause
Idiopathic (no detectable cause) often associated with atrial fibrillation
According to the morphologic abnormality:
Tethering or tenting of TV leaflets
Displacement of the papillary muscles
RV dysfunction/dilation
Annular dilation

RA = right atrium, RV = right ventricle, TV = tricuspid valve.

of low PAP) and RV dilation late in the disease (i.e., in the setting of high PAP) (40).

The TR jet is generally used to estimate RV systolic pressure, using the Bernoulli equation ($4v^2$, where v is the maximum velocity of the TR jet). An estimated RA pressure (based on the size and collapsibility of the inferior vena cava visualized in the subcostal window) is added to the peak systolic pressure gradient of the TR continuous wave spectral Doppler to obtain RV systolic pressure (41). The RV systolic pressure should approximate the systolic pulmonary artery pressure (sPAP) in the absence of pulmonary valve stenosis and RV outflow tract obstruction. A recent large (n = 1,695) single-site study compared Doppler echocardiographic with invasive measurements of sPAP and right atrial pressure (performed within 5 days of each other) in a population of mixed patients (with and without pulmonary hypertension) (42). The correlation between methods was very high ($r = 0.87$; $p < 0.0001$). Bland-Altman analysis showed a bias of −2.0 mm Hg for sPAP (95% confidence limits of agreement [CL]: −18.1 to +14.1 mm Hg) and +1.0 mm Hg for RAP (95% limits of agreement: +0.1 to +1.9 mm Hg). Noninvasive diagnosis of pulmonary hypertension with Doppler echocardiography had a good sensitivity (87%) and specificity (79%), positive and negative predictive values (91% and 70%), as well as accuracy (85%) for an sPAP cutoff value of 36 mm Hg (area under the curve [AUC]: 0.91; $p < 0.001$; 95% confidence interval [CI]: 0.90 to 0.93).

PATHOPHYSIOLOGY OF TR

TR can be divided into primary and secondary. Primary TR is relatively rare, and it is the consequence of a primitive lesion of the tricuspid valve due to congenital or acquired disease processes that affect the leaflets or chordal structures, or both. Secondary TR is more common and is secondary to other diseases such as left-side heart diseases, pulmonary hypertension, RV dilation, and dysfunction from any cause, without intrinsic lesion of the TV itself. The causes of primary and secondary TR are summarized in Table 1.

PRIMARY TR. Primary TR can be the result of congenital disorders such as Ebstein's anomaly or acquired diseases of the TV such as myxomatous degeneration of the tricuspid valve leading to TV prolapse, endocarditis, carcinoid syndrome, rheumatic disease, radiation, and trauma. Although primary TR is relatively rare compared to secondary TR, it should be recognized and distinguished from secondary TR, which is crucial for patient selection and clinical decision making.

PATHOPHYSIOLOGY OF SECONDARY (FUNCTIONAL) TR. The most common cause of TR is secondary or "functional" regurgitation. Secondary TR (STR) can be categorized either by the underlying cause or by the morphologic abnormality of the tricuspid apparatus; some morphologies are clearly associated with specific underlying diseases. If classified by underlying disease, STR can be divided into the following 4 types: 1) STR because of the left-sided heart disease (valve disease or left ventricular dysfunction); 2) STR because of any cause of pulmonary arterial hypertension (chronic lung disease, pulmonary thromboembolism, left-to-right shunt disease, or Doppler estimated systolic pulmonary artery pressure of >50 mm Hg without an identifiable clinical cause); 3) STR because of any cause of RV dysfunction (myocardial disease or RV ischemia/infarction); and 4) STR with no detectable cause of TR (idiopathic STR). The morphologic abnormalities associated with STR, which can occur together include 1) tethering or tenting of the tricuspid leaflets, 2) displacement of the papillary muscles, 3) RV dysfunction, and 4) dilation of the annulus and/or RA (Central Illustration).

The most common causes of STR are left-sided valve disease (primarily mitral disease), LV and RV cardiomyopathy (ischemic and nonischemic), and RV

TABLE 2 Anatomic Considerations for Surgical or Transcatheter Interventions

Tricuspid Leaflets and Commissures	Interventional Considerations
• Large valve orifice (~9 cm^2, with mean gradient <2 mm Hg) • Usually 3 leaflets but variable (up to 6) or with deep clefts and folds • Very thin, translucent leaflets • The anterior leaflet is typically the largest, with the greatest motion • Septal leaflet may be short radially, and is the least mobile	• Stenosis is unlikely with central orifice devices (i.e., edge-to-edge repair or spacer devices); however, mean gradients of >2-3 mm Hg may be significant. • Imaging leaflet anatomy may be challenging • Imaging leaflet anatomy challenging • Leaflets may not be ideal for anchoring devices • High leaflet stress occurs with greater leaflet motion • Maneuvering to capture this leaflet may be difficult
Chordae and Papillary Muscles	**Interventional Considerations**
• The anterior papillary muscle is the largest, supplying chordal support to the anterior and posterior leaflets • Septal leaflet chordae insert directly into the septum or with multiple, small papillary muscles • An average of 25 chordae with various configurations composed of straight collagen bundles (thus less distensible than mitral chordae)	• The anterior papillary muscle serves as an imaging landmark for these leaflets • "Tenting" or tethering of the septal leaflet is a common cause of secondary TR, particularly if the septum is displaced toward the left ventricle • Chordae may interact with catheters and devices. Marked tethering results from dilation of the right ventricle or displacement of papillary muscles
Tricuspid Annulus	**Interventional Considerations**
• D-shaped and flat along the septum • Dynamic (larger in end-systole, early diastole, and atrial systole) • Average perimeter = 12 ± 1 cm Average area = 11 ± 2 cm^2 • Heterogeneity in muscle and fatty tissues with discontinuous fibrous support	• Dilation in disease states occurs along the unsupported lateral and posterior free wall portion of the annulus with more planar, circular shape. • Dynamic changes in shape must be accounted for with device design • In the setting of dilation, large annular devices may be required • Stability of annular anchoring systems may vary along the circumference of the annulus
Structures Adjacent to the Tricuspid Valve	**Interventional Considerations**
• Right atrium is thin-walled, markedly dilated in advanced disease • SVC = mean length ~7 cm, maximum diameter ~2 cm, irregular in shape • IVC = largest vein in the body (normally <21 mm) • Coronary sinus enters right atrium at the commissure between the septal and posterior leaflet • No continuity between inflow and outflow • Right coronary artery within the AV groove (variable transverse distance from annulus) • AVN, bundle of His crosses the septal leaflet attachment 3 to 5 mm posterior to the anteroseptal commissure • Noncoronary sinus of Valsalva borders the anterior/superior annulus (commissure between the noncoronary/right coronary sinuses adjacent to the septal/anterior tricuspid leaflet commissure)	• Large space to maneuver devices but more difficult for imaging • Venous access considerations for new devices may be limited by SVC diameters and nonlinear shape. IVC-annular angle may pose issues for device placement • Inflow of the coronary sinus is a good anatomic marker of this commissure • Little risk for outflow tract obstruction • Short (~3-4 mm) transverse distance along the inferior annulus (adjacent to the posterior leaflet) • Risk for heart block with devices in this region • Risk for perforation with devices in this region • Aortic sinuses of Valsalva may be used as an anatomic marker for the septal-anterior commissure

AVN = atrioventricular node; IVC = inferior vena cava; SVC = superior vena cava; TR = tricuspid regurgitation.

dilation due to pulmonary disease (cor pulmonale) (43,44). Left-sided heart disease, especially mitral regurgitation or stenosis and heart failure from various causes (17,45), is associated commonly with elevated left atrial filling pressure, subsequent pulmonary venous hypertension, or increased pulmonary vascular resistance associated with pulmonary arterial hypertension. This may result in dilation and lengthening of the RV (with or without RV dysfunction) and dilation of the RA/tricuspid annulus. In some cases, RV dysfunction/dilation can be secondary to primary disease of the RV muscle (ischemic or other cardiomyopathic processes) (10). With RV dilation, especially when the mid RV is dilated, the tricuspid valve leaflets become tethered, with mal coaptation leading to the worsening of TR and then further RV dilation and dysfunction (46,47).

Because the tricuspid regurgitant volume may vary significantly based on loading conditions, TV morphology plays an important role in predicting both TR severity and outcomes with surgical annular repairs. Specifically, tenting areas and volumes correlate with TR severity and with outcomes following surgical repair (48-51). Tethering of the tricuspid leaflets is thought to be sufficient to cause TR, even in the absence of significant tricuspid annular dilation (52). Tenting areas on echocardiography can be used to predict the severity of regurgitation; multiple studies suggest that >1.0 cm^2 predicts increasingly mild TR (49,53). Tenting volume and the septal leaflet tethering angle are also echocardiographic predictors of TR severity (51). Predictors of post-operative recurrent TR include echocardiographic measurements of tricuspid valve

tenting height of >0.76 cm or tenting area of >1.63 cm^2 (49,53).

Displacement of the papillary muscles due to changes in RV size and shape may also predict TR severity and outcomes (54-56). RV end-systolic area of ≥20.0 cm^2 predicts worse event-free survival (55). End-systolic RV eccentricity index defined from short-axis views as the long axis (largest lateral distance) divided by short axis (septo-free wall distance at the mid-septum) is a predictor of milder TR (55). RV sphericity index, calculated as the RV area divided by RV long-axis dimension (apical view) predicts the tethering height: the greater the sphericity index, the larger the TR regurgitant orifice.

The fourth cause of STR, isolated dilation of the annulus and/or RA in the absence of left-sided disease or pulmonary hypertension, has recently been described. In vitro studies have shown that isolated annular dilation can cause significant tricuspid regurgitation (57). The relationship between TR and age (58) and atrial fibrillation (59) in the absence of other cardiovascular diseases supports the existence of this entity, labeled "idiopathic STR" (60). Idiopathic STR is not associated with significant tethering or tenting of the tricuspid leaflets, and TR is a result of insufficient leaflet coverage of a dilated annulus. Possible contributors to this entity include chronic atrial fibrillation, which may cause dilation of RA and the tricuspid annulus (61-63). A recent 3D echocardiographic study of the 4 causes of STR suggests that the prevalence of idiopathic TR from atrial fibrillation is 9% (59). Interestingly, this study showed an association between atrial fibrillation STR and advanced age, female sex, smaller body surface area, less frequent coronary artery disease, and higher systolic and diastolic blood pressure. Idiopathic STR may indeed be associated with diastolic dysfunction or heart failure with preserved ejection fraction (61), Although the causes of idiopathic STR have not been fully elucidated, natural history studies show outcomes for severe idiopathic STR are poor (65).

ANATOMIC CONSIDERATIONS FOR INTERVENTIONS

Although surgical repair or replacement is the recommended intervention for severe TR, numerous transcatheter devices are currently in early clinical trials or being developed (64). There are multiple considerations that require a comprehensive understanding of right-heart anatomy. First, there are multiple access sites possible for tricuspid valve interventions: vena cavae, direct transatrial and direct transapical. Second, there are multiple ways of anchoring the devices: annulus, leaflets, vena cavae, myocardium. Third, adjacent anatomy should be considered to avoid complications or, sometimes, to help guide the procedures. Finally, the understanding of anatomy may help with device selection based on the specific pathophysiology of the disease in an individual patient. **Table 2** lists the anatomy and relevant considerations for interventions on the tricuspid valve.

CONCLUSIONS

STR may result from a number of disease processes in which the different components of the tricuspid apparatus may be involved, in combination or individually, and without a significant primary lesion of the tricuspid valve. A comprehensive understanding of the normal tricuspid valve anatomy is integral to understanding the pathophysiology behind failure of tricuspid leaflet coaptation. In addition, as we interventions move toward transcatheter solutions for functional TR, familiarity with this complex anatomy will be essential.

ADDRESS FOR CORRESPONDENCE: Dr. Rebecca T. Hahn, Columbia University Medical Center, New York-Presbyterian Hospital, 177 Fort Washington Avenue, New York, New York 10032. E-mail: rth2@columbia.edu.

REFERENCES

1. Nath J, Foster E, Heidenreich PA. Impact of tricuspid regurgitation on long-term survival. J Am Coll Cardiol 2004;43:405-9.

2. Neuhold S, Huelsmann M, Pernicka E, et al. Impact of tricuspid regurgitation on survival in patients with chronic heart failure: unexpected findings of a long-term observational study. Eur Heart J 2013;34:844-52.

3. Calafiore AM, Gallina S, Iaco AL, et al. Mitral valve surgery for functional mitral regurgitation: should moderate-or-more tricuspid regurgitation be treated? A propensity score analysis. Ann Thorac Surg 2009;87:698-703.

4. Dahou A, Magne J, Clavel MA, et al. Tricuspid regurgitation is associated with increased risk of mortality in patients with low-flow low-gradient aortic stenosis and reduced ejection fraction: results of the multicenter TOPAS study (True or Pseudo-Severe Aortic Stenosis). J Am Coll Cardiol Intv 2015;8:588-96.

5. Taramasso M, Maisano F, De Bonis M, et al. Prognostic impact and late evolution of untreated moderate (2/4+) functional tricuspid regurgitation in patients undergoing aortic valve replacement. J Cardiac Surg 2016;31:9-14.

6. Xanthos T, Dalivigkas I, Ekmektzoglou KA. Anatomic variations of the cardiac valves and papillary muscles of the right heart. Ital J Anat Embryol 2011;116:111-26.

7. Martinez RM, O'Leary PW, Anderson RH. Anatomy and echocardiography of the normal and abnormal tricuspid valve. Cardiol Young 2006;16 Suppl 3:4-11.

8. Fawzy H, Fukamachi K, Mazer CD, et al. Complete mapping of the tricuspid valve apparatus using three-dimensional sonomicrometry. J Thorac Cardiovasc Surg 2011;141:1037–43.

9. Hahn RT. State-of-the-Art Review of echocardiographic imaging in the evaluation and treatment of functional tricuspid regurgitation. Circ Cardiovasc Imaging 2016;9. pii: e005332.

10. Rodés-Cabau J, Hahn RT, Latib A, et al. Transcatheter therapies for treating tricuspid regurgitation. J Am Coll Cardiol 2016;67:1829–45.

11. Taramasso M, Pozzoli A, Basso C, et al. Compare and contrast tricuspid and mitral valve anatomy: interventional perspectives for transcatheter tricuspid valve therapies. EuroIntervention 2018;13:1889–98.

12. Fukuda S, Saracino G, Matsumura Y, et al. Three-dimensional geometry of the tricuspid annulus in healthy subjects and in patients with functional tricuspid regurgitation: a real-time, 3-dimensional echocardiographic study. Circulation 2006;114:I492–8.

13. Antunes MJ, Barlow JB. Management of tricuspid valve regurgitation. Heart 2007;93:271–6.

14. Shah PM, Raney AA. Tricuspid valve disease. Curr Probl Cardiol 2008;33:47–84.

15. Kostucki W, Vandenbossche JL, Friart A, Englert M. Pulsed Doppler regurgitant flow patterns of normal valves. Am J Cardiol 1986;58:309–13.

16. Anwar AM, Geleijnse ML, Soliman OI, et al. Assessment of normal tricuspid valve anatomy in adults by real-time three-dimensional echocardiography. Int J Cardiovasc Imaging 2007;23:717–24.

17. Rogers JH, Bolling SF. The tricuspid valve: current perspective and evolving management of tricuspid regurgitation. Circulation 2009;119:2718–25.

18. Silver MD, Lam JHC, Ranganathan N, Wigle ED. Morphology of the human tricuspid valve. Circulation 1971;43:333–48.

19. Tretter JT, Sarwark AE, Anderson RH, Spicer DE. Assessment of the anatomical variation to be found in the normal tricuspid valve. Clin Anat 2016;29:399–407.

20. Karas S Jr., Elkins RC. Mechanism of function of the mitral valve leaflets, chordae tendineae and left ventricular papillary muscles in dogs. Circ Res 1970;26:689–96.

21. Lim KO. Mechanical properties and ultrastructure of normal human tricuspid valve chordae tendineae. Jpn J Physiol 1980;30:455–64.

22. Messer S, Moseley E, Marinescu M, Freeman C, Goddard M, Nair S. Histologic analysis of the right atrioventricular junction in the adult human heart. J Heart Valve Dis 2012;21:368–73.

23. Ton-Nu TT, Levine RA, Handschumacher MD, et al. Geometric determinants of functional tricuspid regurgitation: insights from 3-dimensional echocardiography. Circulation 2006;114:143–9.

24. Dreyfus GD, Corbi PJ, Chan KM, Bahrami T. Secondary tricuspid regurgitation or dilation: which should be the criteria for surgical repair? Ann Thorac Surg 2005;79:127–32.

25. Mahmood F, Kim H, Chaudary B, et al. Tricuspid annular geometry: a three-dimensional transesophageal echocardiographic study. J Cardiothorac Vasc Anesth 2013;27:639–46.

26. Ueda A, McCarthy KP, Sanchez-Quintana D, Ho SY. Right atrial appendage and vestibule: further anatomical insights with implications for invasive electrophysiology. Europace 2013;15:728–34.

27. Diez-Villanueva P, Gutierrez-Ibanes E, Cuerpo-Caballero GP, et al. Direct injury to right coronary artery in patients undergoing tricuspid annuloplasty. Ann Thorac Surg 2014;97:1300–5.

28. Vollroth M, Sandri M, Garbade J, Mohr FW. Severe right coronary artery injury during minimally invasive tricuspid valve repair. Eur J Cardiothorac Surg 2015;48:e62.

29. Rudski LG, Lai WW, Afilalo J, et al. Guidelines for the echocardiographic assessment of the right heart in adults: a report from the American Society of Echocardiography endorsed by the European Association of Echocardiography, a registered branch of the European Society of Cardiology, and the Canadian Society of Echocardiography. J Am Soc Echocardiogr 2010;23:685–713. quiz 786–8.

30. Mahlon MA, Yoon HC. CT angiography of the superior vena cava: normative values and implications for central venous catheter position. J Vasc Interv Radiol 2007;18:1106–10.

31. Sonavane SK, Milner DM, Singh SP, Abdel Aal AK, Shahir KS, Chaturvedi A. Comprehensive imaging review of the superior vena cava. Radiographics 2015;35:1873–92.

32. Lin FY, Devereux RB, Roman MJ, et al. The right sided great vessels by cardiac multidetector computed tomography: normative reference values among healthy adults free of cardiopulmonary disease, hypertension, and obesity. Acad Radiol 2009;16:981–7.

33. Steding-Ehrenborg K, Arvidsson PM, Toger J, et al. Determinants of kinetic energy of blood flow in the four-chambered heart in athletes and sedentary controls. Am J Physiol Heart Circ Physiol 2016;310:H113–22.

34. Arvidsson PM, Toger J, Heiberg E, Carlsson M, Arheden H. Quantification of left and right atrial kinetic energy using four-dimensional intracardiac magnetic resonance imaging flow measurements. J Appl Physiol 2013;114:1472–81.

35. Arvidsson PM, Toger J, Carlsson M, et al. Left and right ventricular hemodynamic forces in healthy volunteers and elite athletes assessed with 4D flow magnetic resonance imaging. Am J Physiol Heart Circ Physiol 2017;312:H314–28.

36. Haddad F, Hunt SA, Rosenthal DN, Murphy DJ. Right ventricular function in cardiovascular disease, part I: anatomy, physiology, aging, and functional assessment of the right ventricle. Circulation 2008;117:1436–48.

37. Dell'Italia LJ. Anatomy and physiology of the right ventricle. Cardiol Clin 2012;30:167–87.

38. MacNee W. Pathophysiology of cor pulmonale in chronic obstructive pulmonary disease. Part One. Am J Respir Crit Care Med 1994;150:833–52.

39. Bartelds B, Borgdorff MA, Smit-van Oosten A, et al. Differential responses of the right ventricle to abnormal loading conditions in mice: pressure vs. volume load. Eur J Heart Fail 2011;13:1275–82.

40. De Meester P, Van De Bruaene A, Herijgers P, Voigt JU, Delcroix M, Budts W. Geometry of the right heart and tricuspid regurgitation to exclude elevated pulmonary artery pressure: new insights. Int J Cardiol 2013;168:3866–71.

41. Lang RM, Badano LP, Mor-Avi V, et al. Recommendations for cardiac chamber quantification by echocardiography in adults: an update from the American Society of Echocardiography and the European Association of Cardiovascular Imaging. J Am Soc Echocardiogr 2015;28:1–39.

42. Greiner S, Jud A, Aurich M, et al. Reliability of noninvasive assessment of systolic pulmonary artery pressure by Doppler echocardiography compared to right heart catheterization: analysis in a large patient population. J Am Heart Assoc 2014;21:3. pii: e001103.

43. Hung J. The pathogenesis of functional tricuspid regurgitation. Semin Thorac Cardiovasc Surg 2010;22:76–8.

44. Di Mauro M, Bezante GP, Di Baldassarre A, et al. Functional tricuspid regurgitation: an underestimated issue. Int J Cardiol 2013;168:707–15.

45. Rodés-Cabau J, Taramasso M, O'Gara PT. Diagnosis and treatment of tricuspid valve disease: current and future perspectives. Lancet 2016;388:2431–42.

46. Spinner EM, Sundareswaran K, Dasi LP, Thourani VH, Oshinski J, Yoganathan AP. Altered right ventricular papillary muscle position and orientation in patients with a dilated left ventricle. J Thorac Cardiovasc Surg 2011;141:744–9.

47. Spinner EM, Lerakis S, Higginson J, et al. Correlates of tricuspid regurgitation as determined by 3D echocardiography: pulmonary arterial pressure, ventricle geometry, annular dilation, and papillary muscle displacement. Circ Cardiovasc Imaging 2012;5:43–50.

48. Sagie A, Schwammenthal E, Padial LR, Vazquez de Prada JA, Weyman AE, Levine RA. Determinants of functional tricuspid regurgitation in incomplete tricuspid valve closure: Doppler color flow study of 109 patients. J Am Coll Cardiol 1994;24:446–53.

49. Fukuda S, Song JM, Gillinov AM, et al. Tricuspid valve tethering predicts residual tricuspid regurgitation after tricuspid annuloplasty. Circulation 2005;111:975–9.

50. Sukmawan R, Watanabe N, Ogasawara Y, et al. Geometric changes of tricuspid valve tenting in tricuspid regurgitation secondary to pulmonary hypertension quantified by novel system with transthoracic real-time 3-dimensional echocardiography. J Am Soc Echocardiogr 2007;20:470–6.

51. Park YH, Song JM, Lee EY, Kim YJ, Kang DH, Song JK. Geometric and hemodynamic determinants of functional tricuspid regurgitation: a real-time three-dimensional echocardiography study. Int J Cardiol 2008;124:160–5.

52. Fukuda S, Gillinov AM, Song JM, et al. Echocardiographic insights into atrial and ventricular

mechanisms of functional tricuspid regurgitation. Am Heart J 2006;152:1208–14.

53. Raja SG, Dreyfus GD. Basis for intervention on functional tricuspid regurgitation. Semin Thorac Cardiovasc Surg 2010;22:79–83.

54. Kim JB, Jung SH, Choo SJ, Chung CH, Lee JW. Clinical and echocardiographic outcomes after surgery for severe isolated tricuspid regurgitation. J Thorac Cardiovasc Surg 2013;146:278–84.

55. Kim YJ, Kwon DA, Kim HK, et al. Determinants of surgical outcome in patients with isolated tricuspid regurgitation. Circulation 2009;120:1672–8.

56. Staab ME, Nishimura RA, Dearani JA. Isolated tricuspid valve surgery for severe tricuspid regurgitation following prior left heart valve surgery: analysis of outcome in 34 patients. J Heart Valve Dis 1999;8:567–74.

57. Spinner EM, Shannon P, Buice D, et al. In vitro characterization of the mechanisms responsible for functional tricuspid regurgitation. Circulation 2011;124:920–9.

58. Singh JP, Evans JC, Levy D, et al. Prevalence and clinical determinants of mitral, tricuspid, and aortic regurgitation (the Framingham Heart Study). Am J Cardiol 1999;83:897–902.

59. Utsunomiya H, Itabashi Y, Mihara H, et al. Functional tricuspid regurgitation caused by chronic atrial fibrillation: a real-time 3-dimensional transesophageal echocardiography study. Circ Cardiovasc Imaging 2017;10:10.1161/CIRCIMAGING.116.004897.

60. Topilsky Y, Khanna A, Le Tourneau T, et al. Clinical context and mechanism of functional tricuspid regurgitation in patients with and without pulmonary hypertension. Circ Cardiovasc Imaging 2012;5:314–23.

61. Topilsky Y, Nkomo VT, Vatury O, et al. Clinical outcome of isolated tricuspid regurgitation. J Am Coll Cardiol Img 2014;7:1185–94.

62. Mutlak D, Lessick J, Reisner SA, Aronson D, Dabbah S, Agmon Y. Echocardiography-based spectrum of severe tricuspid regurgitation: the frequency of apparently idiopathic tricuspid regurgitation. J Am Soc Echocardiogr 2007;20:405–8.

63. Najib MQ, Vinales KL, Vittala SS, Challa S, Lee HR, Chaliki HP. Predictors for the development of severe tricuspid regurgitation with anatomically normal valve in patients with atrial fibrillation. Echocardiography 2012;29:140–6.

64. Mascherbauer J, Kammerlander AA, Zotter-Tufaro C, et al. Presence of isolated tricuspid regurgitation should prompt the suspicion of heart failure with preserved ejection fraction. PloS One 2017;12:e0171542.

65. Rodes-Cabau J, Hahn RT, Latib A, et al. Transcatheter Therapies for Treating Tricuspid Regurgitation. J Am Coll Cardiol 2016;67:1829–45.

KEY WORDS tricuspid regurgitation, tricuspid valve anatomy